Published in final edited form as:
Neurobiol Dis. 2007 April ; 26(1): 14–26.

Impaired spatial learning and defective theta burst induced LTP in mice lacking fibroblast growth factor 14

David F. Wozniak[a,1], **Maolei Xiao**[b,1], **Lin Xu**[c], **Kelvin A. Yamada**[c], and **David M. Ornitz**[b*]

a*Department of Psychiatry, Washington University School of Medicine, St. Louis, MO 63110, USA*

b*Department of Molecular Biology and Pharmacology, Campus Box 8103, Washington University Medical School, 660 S. Euclid Avenue, St. Louis, MO 63110, USA*

c*Department of Neurology, Washington University School of Medicine, St. Louis, MO 63110, USA*

Abstract

Spinocerebellar ataxia 27 (SCA27) is a recently described syndrome characterized by impaired cognitive abilities and a slowly progressive ataxia. SCA27 is caused by an autosomal dominant missense mutation in Fibroblast Growth Factor 14 (FGF14). Mice lacking FGF14 (*Fgf14*$^{-/-}$ mice) have impaired sensorimotor functions, ataxia and paroxysmal dyskinesia, a phenotype that led to the discovery of the human mutation. Here we extend the similarities between *Fgf14*$^{-/-}$ mice and *FGF14 (F145S)* humans by showing that *Fgf14*$^{-/-}$ mice exhibit reliable acquisition (place learning) deficits in the Morris water maze. This cognitive deficit appears to be independent of sensorimotor disturbances and relatively selective since *Fgf14*$^{-/-}$ mice performed similarly to wild type littermates during cued water maze trials and on conditioned fear and passive avoidance tests. Impaired theta burst initiated long-term synaptic potentiation was also found in hippocampal slices from *Fgf14*$^{-/-}$ mice. These results suggest a role for FGF14 in certain spatial learning functions and synaptic plasticity.

Keywords

FGF14; FGF Homologous Factors; Hippocampus; Learning and Memory; LTP; Behavior; Cognition

Introduction

In our initial characterization of mice lacking Fibroblast Growth Factor 14 (FGF14) (Wang et al., 2002), we described existing sensorimotor impairments, ataxia and a paroxysmal hyperkinetic movement disorder. This analysis led directly to the identification of mutations in FGF14 (Brusse et al., 2006; Dalski et al., 2005; Van Swieten et al., 2003) in which affected individuals exhibited a slowly progressive onset of tremors, dyskinesia, and ataxia that were strikingly similar to the phenotype of *Fgf14*$^{-/-}$ mice. Importantly, these patients also exhibited impaired cognitive capabilities, suggesting that FGF14 may play a role in mediating certain cognitive functions. These findings in humans prompted us to examine the learning and memory capabilities and other behaviors in *Fgf14*$^{-/-}$ mice.

FGF14 is a member of the FGF homologous factors subfamily (FHF1–4), and is also known as FHF4. It is expressed in similar brain regions in mice and humans, including the hippocampal CA (Cornu Ammons) subfields, cerebral cortex (temporal lobe), putamen, and pyramidal cell

*Corresponding author. *E-mail address:* dornitz@wustl.edu (D.M. Ornitz).
[1]Authors have contributed equally to this work.

layer of the hippocampus (Wang et al., 2002). Although the complete functions of FGF14 are not known, evidence is beginning to suggest an important role in CNS neuronal physiology (Munoz-Sanjuan et al., 2000; Smallwood et al., 1996; Wang et al., 2002; Yamamoto et al., 1998). Recent work showed that FGF14 could modulate the electrophysiological functions of neurons by modulating voltage-gated sodium (Nav) channel activity (Lou et al., 2005). Furthermore, we found that synaptic transmission at hippocampal Schaffer collateral-CA1 synapses and short and long term modulation are impaired in *Fgf14*$^{-/-}$ mice (Xiao et al., in press). *Fgf14*$^{-/-}$ mice were also observed to have decreased numbers of synaptic vesicles docked at presynaptic CA1 synapses, a significant synaptic fatigue/depression during high/low-frequency stimulation and a reduction in mEPSC frequency, but not amplitude, in cultured hippocampal neurons (Xiao et al., in press).

Here we further explore the similarities between *Fgf14*$^{-/-}$ mice and humans carrying mutations in *FGF14* by examining the learning and memory capabilities and other behaviors in *Fgf14*$^{-/-}$ mice. We show that *Fgf14*$^{-/-}$ mice have acquisition deficits during place trials in the Morris water navigation test that appear to be independent of sensorimotor disturbances since *Fgf14*$^{-/-}$ mice performed similarly to WT littermates during cued trials and have similar swimming speeds. The spatial learning deficits in *Fgf14*$^{-/-}$ mice also appear to be relatively selective since their performance was not impaired relative to WT controls on nonspatial learning/conditioning tasks. We also reexamined LTP in hippocampal slices from *Fgf14*$^{-/-}$ mice using theta burst stimulation, a more physiological LTP induction pattern than tetanic stimulation. LTP maintenance was significantly impaired following theta burst stimulations, similar to what we have found with other types of LTP induction (Xiao et al., in press). Our recent findings provide new perspectives into the possible mechanisms underlying the cognitive deficits in humans with mutations in *FGF14* and suggest that FGF14 may play a role in mediating certain spatial learning functions and regulating hippocampal synaptic plasticity.

Materials and methods

Mice

The *Fgf14* gene was targeted by replacing the second and third exons of *Fgf14* with the β-galactosidase gene. This created a chimeric protein containing the first alternatively spliced exons of FGF14 fused to β-galactosidase (Wang et al., 2002). *Fgf14*$^{-/-}$ mice were maintained on an inbred C57/BL6J background (greater than ten generations of backcrossing to C57/BL6J). All genotypes described were confirmed by PCR analysis (Wang et al., 2002). Littermate or age matched controls were used with littermate controls being used for all behavioral studies.

Behavioral tests

1-h locomotor activity test and sensorimotor battery—General locomotor activity and sensorimotor capabilities were evaluated in the mice before conducting the water navigation experiments in each of the two behavioral studies. Locomotor activity was quantified using a computerized, photobeam system (MotorMonitor, Hamilton-Kinder, LLC, Poway, CA), according to previously published methods (Schaefer et al., 2000; Wozniak et al., 2004), where the number of ambulations (whole body movements) made during a 1-h test period served as the index of activity. To determine possible genotypic differences in sensorimotor capabilities, the mice were evaluated on a battery of tests (inclined and inverted screens, platform, ledge, and pole) designed to assess balance, strength, and coordination, as previously described (Wang et al., 2002; Wozniak et al., 2004).

Grip strength—Forelimb grip strength was evaluated in the mice through the use of a grip strength meter (Stoelting Co., Wooddale, IL) utilizing methods similar to those described by

Connolly et al. (Connolly et al., 2001). The procedure involved placing a mouse over a Perspex plate, in front of a "grasping trapeze", which functions as the arm of a force transducer connected to a peak amplifier. A mouse was taught to grab the trapeze when pulled by the tail until the pulling force overcame its grip strength. After the mouse lost its grip, the peak pull force was measured and stored by the peak preamplifier and shown on a digital display. Our protocol involved 3 days of habituation where each mouse was given a number of trials until it performed 5 "solid" pulls. Testing involved 2, 5-trial sessions with each session being conducted on consecutive days. The dependent variable was pulling force (*g*) for which a mean was computed for each of the 5 trial-test days for each animal.

Rotorod—Motor coordination and balance were evaluated using the rotorod (Rotamex-5, Columbus Instruments, Columbus, OH) test, which involved 3 conditions: a stationary rod (60 s maximum); a rotating rod with a constant speed (5 rpm for 60 s maximum); and a rod which had an accelerating rotational speed (5–20 rpm over 0–180 s). The present protocol was similar to our recently published methods (Grady et al., 2006) in that it was designed to minimize motor learning. This included three testing sessions, each session being separated by 4 days. Each session included 1 trial on the stationary rod, 2 trials on the constant speed rotorod, and 2 trials on the accelerating rotorod. Time spent on the rod in each condition was used as the dependent variable.

Morris water navigation—Spatial learning and memory were evaluated using the Morris water navigation test utilizing procedures similar to previously published methods (Ho et al., 2000; Wozniak et al., 2004). The protocol included cued (visible platform), place (submerged and not visible platform), and probe (platform removed) trials with both escape path length (distance traveled to platform), latency (time taken to reach the platform), and swimming speeds being computed for cued and place trials. All trials were conducted in a round pool (118 cm inner diameter) of opaque water and videotaped. Swim paths were tracked and recorded by a computerized system (Polytrack, San Diego Instruments, San Diego, CA), which calculated escape path length and latency. Mice were first trained on the cued condition to determine if nonassociative factors (e.g., sensorimotor or visual disturbances or alterations in motivation) were likely to affect acquisition performance during subsequent place trials. Mice received 4 trials per day for two consecutive days of cued training, during which time the platform was moved to a different location for each trial within a day in the presence of very few distal cues, thus substantially limiting spatial learning during this time. An inter-trial interval (ITI) of 60 s was used with a mouse being allowed to remain on the platform for 30 s before being removed. Three days later, the mice were trained on the "place" condition to learn the location of a submerged (hidden) platform. The place trials were conducted in the presence of several salient distal cues positioned around the room to facilitate association of the spatial cues with the submerged platform location. During place training, the mice were given 4 trials per day for 5 days (60 s maximum for a trial) with the platform remaining in the same location for all place trials using an ITI of 60 s. The daily protocol involved administering 2 blocks of 2 trials with each block being separated by approximately 2 h. A probe trial was administered approximately 1 h after completion of the place trials on the 5th day to evaluate retention of the platform location. During the 60-s probe trial, the escape platform was removed and a mouse was placed in the quadrant diagonally opposite from the previous platform location. Time spent in the target quadrant where the platform had been, and the number of crossings made over the previous platform location (platform crossings), were recorded. An average proximity score was also calculated during probe trials to help protect against biases from abnormal swimming patterns resulting from sensorimotor disturbances (Gallagher et al., 1993; Magnusson, 1998). The tracking program software automatically calculated this variable by sampling the position of the mouse in the pool several times per second to compute the distances between the mouse and the middle of the escape platform location and then by

averaging the distances for 1 s intervals. These values were then averaged over the 60 s probe trial. In general, higher proximity scores indicate search patterns that are more distant from the platform location.

For the behavioral studies, mature adult and middle-aged mice were used to minimize the effects of paroxysmal dyskinesia in *Fgf14*$^{-/-}$ mice since we have observed episodes of dyskinesia to decrease significantly with increasing age. Study 1 was conducted on groups of male *Fgf14*$^{-/-}$ (*n*=11) mice and WT (*n*=11) littermate controls that were 6–8 months of age. Study 2 was conducted on naive male *Fgf14*$^{-/-}$ (*n*=7) mice and WT littermates (*n*=8) that were 8–9 months old. A second water navigation experiment (study 2B) was conducted on these same groups of mice 2 months after the first study was completed using the same procedures described above except that a different submerged platform location was used during the place trials and different (but equally salient) distal cues were used as well.

Step-through passive avoidance—Testing was carried out in an apparatus containing an illuminated (light) and a dark compartment separated by a sliding door, using a protocol similar to one described by Nabeshima et al., (Nabeshima et al., 1999). During acquisition trials, individual mice were placed in the light chamber, and 10 s later, the door to the dark compartment was opened. When the mouse stepped with all four paws into the dark compartment, the door was closed and the step-through latency was recorded. The mouse was removed from the dark chamber after receiving the foot shock (0.2 mA, 2 s) and was placed back into the light compartment and the door was opened after 10 s to start the next trial. Acquisition training continued until a mouse stayed in the light compartment (without going into the dark-shock chamber) for 120 s during a given trial. Twenty-four hours after reaching the acquisition criterion, a retention trial was administered by placing the mouse in the light compartment and recording the step-through latency, during which time no shocks were administered. The mice were also tested again 24 h later (i.e., 48 h post acquisition) to determine possible differences in extinction. The maximum time for the retention/extinction trials if the mouse did not enter the dark compartment was 300 s.

Conditioned fear (contextual and auditory cue tests)—Mice were evaluated on the conditioned fear test according to previously published methods (Khuchua et al., 2003) except that in the present study, freezing behavior was scored by a computerized video-based image analysis system (see below). Briefly, the mice were trained and tested in two-*Plexiglas* conditioning chambers (26 cm × 18 cm, and 18 cm high) (Med-Associates, St. Albans, VT) with each chamber differing in terms of odor, visual and tactile cues. On the day before testing, the mice were placed into the training chamber for 10 min to habituate them to handling and the apparatus. Twenty-four hours later, each mouse was placed into the conditioning chamber for 5 min. Freezing behavior was quantified during a 2 min baseline period, after which an 80 dB tone (conditioned stimulus; CS) consisting of broadband white noise was presented for 20 s. Broadband white noise was used instead of a frequency-specific tone in an effort to avoid possible auditory deficits that might occur with age. During the last second of the pulse, the mice received a 1.0 mA continuous foot shock (unconditioned stimulus; US). This CS-US (tone-shock) pairing was repeated each minute over the next 2 min. The mice were removed from the testing chamber 40 s after the third shock and returned to their home cages. Twenty-four hours later, each mouse was placed in the same conditioning chamber in which it was trained to test contextual fear, which involved quantifying freezing behavior for 8 min. Twenty-four hours later, each mouse was placed in the other conditioning chamber to be evaluated on the auditory cue test. The mice were observed for 10 min in this “altered context” and freezing behavior was quantified during a 2 min baseline period and over a subsequent 8 min period, during which time the auditory cue (tone; CS) was presented. Freezing was quantified using *FreezeFrame* image analysis software (Actimetrics, Evanston, IL) which allowed for simultaneous visualization of behavior while adjusting a “freezing threshold,” which

categorized behavior as freezing or not freezing during 0.75 s intervals. Freezing was defined as no movement except for that associated with normal respiration, and the data were presented as percent of time spent freezing.

Histology

Perfusion and histochemical analysis—Mice were anesthetized with sodium pentobarbital (60 mg/kg, i.p.) and transcardially perfused with a vascular rinse of 0.9% NaCl followed by ice-cold 4% paraformaldehyde in 0.1 M phosphate buffer. Brains were dissected, postfixed in the same solution overnight at 4 °C, and cryoprotected in 30% sucrose in 0.1 M phosphate buffer until they sank. After embedding in O. C. T. compound, brains were cryosectioned at 14 μm or 30 μm and collected in PBS for immunostaining and in situ hybridization. For histochemical analysis, sections were stained with 0.1% cresyl violet according to standard procedures.

X-gal staining—500 μm sections were cut with a vibratome in ice-cold X-gal rinse buffer (0.1 M PBS and 2 mM MgCl2), and then fixed for 1 h in 0.5% glutaraldehyde in X-gal rinse buffer at 4 °C. The sections were stained in X-gal staining solution (20 mM potassium ferricyanide, 20 mM potassium ferrocyanide, 0.02% Nonidet P-40, 0.01% sodium deoxycholate, and 1 mg/ml 5-bromo-4-chloro-3-indoyl-β-D-galactosidase made up in rinse buffer, pH 7.6) overnight at 37 °C to reveal transgene-expressing cells in the brain. After X-gal staining, the sections were cryoprotected in 30% sucrose in 0.1 M phosphate buffer until they sank, embedded in O. C. T. compound, and cryosectioned at 14 μm. The sections were dehydrated in an ethanol series, then in xylene, and then mounted in DPX mount (BDH Chemicals).

Immunohistochemistry and in situ hybridization—For immunohistochemistry, free-floating brain sections (14 μm) were washed in PBS, blocked in a solution of 7.5% goat serum (Sigma) and 0.25% Triton X-100 (TX-100; Sigma) in PBS. Sections were then incubated at 4 °C overnight with the primary antibodies diluted in 1% goat serum/0.25% TX-100 in PBS. The following specific antibodies were used: mouse anti-GFAP (Sigma) at 1:500, rat anti-CaM Kinase II (Affinity BioReagents) at 1:1000, mouse anti-PKCγ (BD biosciences) at 1:1000, mouse anti-synaptophysin (Chemicon) at 1:1000, goat anti-SNAP-25 (Chemicon) at 1:1000. Sections were then washed three times for 5 min at room temperature in PBS before application of secondary antibodies. Sections were then incubated in the appropriate secondary goat or rabbit antibodies (labeled with Alexa 488 or Texas Red) against either mouse, rat or goat. Secondary antibodies were diluted in the same solution as the primary antibodies.

For in situ hybridization, a 550 bp RNA probe (Wang et al., 2000) was labeled with digoxigenin following the manufacturer's protocol (Roche Diagnostics, IN). Free-floating brain sections (30 μm) were washed twice in PBS and treated with freshly prepared 10 μg/ml proteinase K (Invitrogen, Carlsbad, CA) at 37 °C. After acetylation, sections were incubated in hybridization buffer containing 0.2 μg/ml digoxigenin-labeled riboprobes at 43 °C overnight. Hybridized sections were washed by successively immersing them in 4× SSC (150 mM NaCl, 15 mM sodium citrate, pH 7.0, room temperature), 2× SSC containing 50% formamide (50 °C, 30 min), 2× SSC (37 °C, 10 min), 2× SSC containing 20 μg/ml RNase A (37 °C, 30 min), 2× SSC (37 °C, 20 min), and 0.1× SSC (room temperature, 10 min). The hybridization signals were detected with digoxigenin detection reagents (Roche Diagnostics, Indianapolis, IN). After rinsing in PBS, sections were mounted and analyzed with a Zeiss Axioskop microscope.

Electrophysiology

Preparation of hippocampal slices and recording—Two to 3-month-old WT and *Fgf14*$^{-/-}$ littermates were used in all electrophysiological experiments. After halothane

anesthesia, decapitation, and removal of the brain, transverse acute hippocampal slices (400 μm) were cut with a vibratome in ice-cold artificial CSF (ACSF) containing 124 mM NaCl, 5 mM KCl, 2.5 mM $CaCl_2$, 2 mM $MgSO_4$, 1.25 mM NaH_2PO_4, 22 mM $NaHCO_3$, 10 mM glucose. The slice preparation and protocol for electrical stimulation and recordings were as described (Yamada et al., 2004). The slices were kept for at least 1 h before recording at room temperature in 95% O_2 and 5% CO_2 bubbled ACSF. Orthodromic field EPSPs (fEPSP) were evoked with 100–200 μs constant current pulses applied to the Schaffer collateral pathway via a tungsten bipolar electrode. The stimulus intensity utilized produced an fEPSP with half-maximal amplitude. To induce LTP, 3 theta burst stimuli (3TB) were applied using this stimulus intensity (Diano et al., 2006). The fEPSP was recorded from stratum radiatum in the CA1 subfield with glass pipettes filled with 2 M NaCl (5–10 MΩ DC resistance) connected to an Axoclamp2A amplifier (Molecular Devices, Union City, CA). Traces were digitized using Clampex 9 and a Digidata 1322A interface and the data were analyzed using Clampfit 9.0 (PClamp software, Molecular Devices, Union City, CA). For LTP experiments, the average slope of the fEPSPs during a 20 min baseline recording period was used to normalize the fEPSP slopes in order to combine data from different slices for group comparisons. Average responses (mean±SEM) were expressed as percent of baseline response.

Statistical analyses—Analysis of variance (ANOVA) models were used when possible to analyze the data. ANOVA models containing one between-subjects variable (genotype) and one within-subjects (repeated measures) variable (e.g., blocks of trials) were used to analyze the behavioral data. The Huynh–Feldt adjustment of alpha levels was utilized for all within-subjects effects containing more than two levels to protect against violations of sphericity/compound symmetry assumptions. Bonferroni correction was used to help maintain alpha levels at 0.05 when multiple comparisons were conducted.

Results

Expression of FGF14 in parahippocampal regions and the amygdala

Although *Fgf14* is widely expressed in the developing and adult CNS (Smallwood et al., 1996; Wang et al., 2002), the precise locations of *Fgf14* mRNA and protein in the adult CNS is still unclear. β-gal, which was inserted in the *Fgf14* gene, was expressed in neurons in the olfactory mitral cell layer, cerebral cortex, hippocampus, thalamic nuclei, amygdaloid nuclei, red nuclei, deep cerebellar nuclei, and cranial nerve nuclei located in the pons, medulla, olive and spinal cord (Fig. 1A and data not shown). The β-gal expression pattern in the adult CNS correlated well with that of *Fgf14* determined by *in situ* hybridization in mice and by RNA blot analysis of human brain regions (Fig. 1D and Wang et al., 2002). To determine localized expression patterns of *Fgf14* that may be relevant to learning and memory functions, we examined major CNS regions including the hippocampus, parahippocampal region (PHR) and amygdala, using *in situ* hybridization and β-galactosidase (β-gal). In the hippocampus, the FGF14-β-gal expression pattern was consistent with expression in both principal cells and interneurons of CA1, CA3 and the dentate gyrus (DG) (Xiao et al., in press). In the PHR, including the entorhinal, perirhinal and postrhinal cortex, β-gal expression was clearly seen in layers II through VI of the perirhinal cortex (PRh), lateral (LEnt) and medial entorhinal cortex, piriform cortex (Pir) and dorsal endopiriform nucleus (DEn) (Fig. 1B). In the amygdale, β-gal was expressed in nuclei including the dorsolateral amygdaloid nucleus (LaDL), the anterior basolateral amygdaloid nucleus (BLA) and the anterior basolateral amygdala (BMA) (Fig. 1C). High resolution *in situ* detection of the *Fgf14* mRNAin 2- to 3-month-old WT mice showed a regional distribution pattern closely paralleling the β-Gal expression pattern seen in *Fgf14*$^{-/+}$ mice (Figs. 1E, F). The prominent expression of *Fgf14* in the hippocampus and in its related major projections suggest that *Fgf14* may play a role in mediating learning and memory functions.

Behavioral deficits in Fgf14$^{-/-}$ mice

Initial characterization of the behavioral phenotype of *Fgf14*$^{-/-}$ mice focused on their ataxia and sensorimotor deficits, which were thought to be related to the absence of FGF14 in the striatum and cerebellum (Wang et al., 2002). Since FGF14 expression was also observed in the hippocampus and neocortex, and humans with mutations in *Fgf14* exhibit impaired cognitive functions (Brusse et al., 2006; Dalski et al., 2005; Van Swieten et al., 2003), we hypothesized that *Fgf14*$^{-/-}$ mice may also have compromised cognitive capabilities. To test this hypothesis, we assessed specific learning and memory capabilities in *Fgf14*$^{-/-}$ and WT littermates by evaluating them on a spatial learning and memory task (Morris water navigation test) and on two nonspatial tasks (passive avoidance and conditioned fear). Data from the cued condition of the water navigation test, as well as those from other behavioral measures (activity, sensorimotor battery, rotorod), were used to assess whether certain nonassociative behavioral disturbances (e.g., impaired vision, sensorimotor deficits, altered motivation) were likely to affect learning and memory performance.

Hyperactivity and sensorimotor, rotorod, and grip strength deficits in Fgf14$^{-/-}$ mice

In two independent studies from the present work, *Fgf14*$^{-/-}$ mice were found to be hyperactive, exhibiting significantly more ambulations (whole body movements) than WT controls during a 1 h test period, [$F(1,20)=22.9$, $p<0.005$ and $F(1,13)=11.5$, $p=0.005$] (Fig. 2A). With regard to the results from the sensorimotor battery, inbred *Fgf14*$^{-/-}$ mice exhibited impaired performance in one, but not both, behavioral studies for the ledge, pole, and 60° and 90° inclined screen tests (data not shown). However, consistent with our previous work with mice on an outbred genetic background (Wang et al., 2002), inbred *Fgf14*$^{-/-}$ mice were significantly impaired on the platform and inverted screen measures of the battery during each of the two behavioral studies, and on both the constant speed and accelerating rotorod (data not shown). We chose not to show the data from the sensorimotor battery or rotorod test since it is very similar to data presented in our initial paper involving mice on an outbred background (Wang et al., 2002). However, the consistency of the impaired performance of *Fgf14*$^{-/-}$ mice on the inverted screen test suggested that at least some portion of the sensorimotor deficits in these mice may be due to deficits in grip strength. This was confirmed for the forelimbs by our experiment involving the measurement of this variable using a grip strength meter. These results showed that inbred *Fgf14*$^{-/-}$ mice consistently exhibited significantly reduced forelimb strength in gripping the bar of the test apparatus (Fig. 2B), as indicated by a significant main effect of genotype [$F(1,20)=21.1$, $p<0.0005$], and by subsequent pairwise comparisons documenting significant differences in grip strength being present on both Test Day 1 and Day 2 [$F(1,20)=17.9$, $p<0.0005$; and $F(1,20)=19.2$, $p<0.0005$, respectively].

In summary, inbred *Fgf14*$^{-/-}$ mice in the present studies were found to have similar phenotypes compared to outbred mice examined previously (Wang et al., 2002), although the extent of sensorimotor impairment in the inbred *Fgf14*$^{-/-}$ mice may be slightly less than originally observed in the outbred strain. Note that although inbred *Fgf14*$^{-/-}$ mice were found to be ataxic and to have certain sensorimotor deficits, these impaired functions did not prevent them from showing locomotor hyperactivity relative to WT littermate controls. Careful, subsequent study was required to determine whether these compromised functions in *Fgf14*$^{-/-}$ mice were likely to affect performance on the learning and memory tests, apart from any cognitive disturbances in these mice.

Impaired spatial learning in Fgf14$^{-/-}$ mice

Fgf14$^{-/-}$ and WT littermate control mice were evaluated on the water navigation test in two separate studies (studies 1 and 2) involving different groups of animals for each study. In study 1, data from the cued trials showed no significant difference between *Fgf14*$^{-/-}$ and control mice in terms of escape path length (Fig. 3A). However, the *Fgf14*$^{-/-}$ mice exhibited

significantly longer escape latencies in navigating to the visible platform compared to the WT mice [$F(1,20)=6.9$, $p=0.02$] (data not shown). This difference could be attributed to slower swimming speeds in *Fgf14*$^{-/-}$ mice (data not shown) [$F(1,20)=20.6$, $p<0.0005$)]. These data showed that despite somewhat compromised swimming abilities, the path lengths in navigating to the visible platform were not aberrant in *Fgf14*$^{-/-}$ mice compared to controls. In contrast to the path length data from the cued trials, the acquisition performance of the *Fgf14*$^{-/-}$ mice was significantly impaired during the place condition. Specifically, a significant main effect of genotype [$F(1,20)=20.4$, $p<0.0005$], indicated that, on the average, the *Fgf14*$^{-/-}$ mice had significantly longer path lengths in locating the submerged platform compared to WT controls (Fig. 3B). Control mice also showed significant improvement in path length scores during Block 5 compared to Block 1 [$F(1,20)=15.8$, $p=0.001$], suggesting that learning had occurred. The *Fgf14*$^{-/-}$ mice showed no such evidence of learning. The *Fgf14*$^{-/-}$ mice also had significantly longer escape latencies [$F(1,20)= 19.3$, $p<0.0005$] (Fig. 3C), some portion of which may be attributed to slower swimming speeds (Fig. 4A). Retention performance of the groups during the probe trial did not reveal a significant difference between *Fgf14*$^{-/-}$ and control mice (Fig. 3I). The *Fgf14*$^{-/-}$ mice also made fewer crossings over the former platform location and exhibited higher average proximity scores, but these differences did not achieve statistical significance (data not shown).

To confirm these results, we performed a second study in which two additional water navigation experiments were conducted (study 2 and 2B) on a different group of naive mice. In study 2, analysis of the data from the cued trials indicated that the *Fgf14*$^{-/-}$ and WT mice did not differ in their performance with reference to escape path length, latency, or swimming speeds (Fig. 3D and data not shown). However, similar to the results from study 1, the mice exhibited impaired acquisition performance during the place trials (Fig. 3E), as indicated by a significant main effect of genotype for escape path length [$F(1,13)=17.4$, $p=0.001$]. Differences between the groups were particularly large during the 3rd block of trials [$F(1,13)=10.3$, $p=0.007$], where they exceeded Bonferroni levels ($p=0.01$). Similar results were found for escape latency (Fig. 3F): (1) significant main effect of genotype [$F(1,13)=14.9$, $p=0.002$]; (2) Block 3 differences (pairwise comparison) [$F(1,13)=8.6$, $p=0.011$]. Importantly, no differences were found between groups in terms of swimming speeds (Fig. 4B). Analysis of the probe trial data indicated that the *Fgf14*$^{-/-}$ and control groups did not differ on time in the target quadrant (Fig. 3K), platform crossings, or average proximity scores (not shown), although both groups exhibited good retention of the submerged platform location, as shown by their spatial bias for the target quadrant (Fig. 3K).

The same groups of mice were retested 2 months after the completion of study 2 to determine their ability to learn a new submerged platform location in the presence of different distal spatial cues (study 2B). The results of the place trials in study 2B (Figs. 3G and H) were very similar to those from study 2 in that a significant main effect of genotype was found for both path length and latency [$F(1,13)=9.3$, $p=0.009$; and $F(1,13)=5.9$, $p=0.03$, respectively], thus documenting generally-impaired performance across blocks of trials on the part of the *Fgf14*$^{-/-}$ mice to learn new platform locations. Consistent with the results from study 2, there were no differences in swimming speeds during the place trials (Fig. 4C). However, analysis of the probe trial data (Fig. 3J) showed that the WT mice spent significantly more time in the target quadrant and had significantly lower average proximity scores [$F(1,13)=25.4$, $p<0.0005$, $F(1,13)=21.0$, $p=0.001$, respectively], compared to the *Fgf14*$^{-/-}$ mice. The WT mice also made more crossings over the former platform location, but these differences were not statistically significant (not shown). In addition, the groups did not differ in terms of total swimming distance during this probe trial (not shown), suggesting that the spatial bias was not an artifact resulting from compromised swimming abilities. Collectively, our data from three experiments show that male *Fgf14*$^{-/-}$ mice have reliable spatial learning (acquisition) performance deficits

that are not likely due to nonassociative factors (e.g., visual or sensorimotor disturbances, or alterations in motivation).

The impaired performance of the *Fgf14*$^{-/-}$ mice on the two probe trial variables in study 2B suggested that these mice might have subtle retention deficits as well as disturbed acquisition capabilities. However, these retention deficits may be subtle enough to require increasing the memory demands of the spatial learning task to become demonstrable. In this regard, we reasoned that testing the mice after an interval of 24 h between acquisition (place) trials might reveal performance deficits on the part of the *Fgf14*$^{-/-}$ mice that were not observable with shorter intervals. Therefore, we reanalyzed some of the data from studies 1 and 2 in different ways to test this hypothesis. Specifically, average place trial performances, in terms of escape path length of the *Fgf14*$^{-/-}$ and WT mice during trial 1 across test days 2, 3, 4, 5, where there was a 24 h interval between trials, were compared. Additionally, average place trial performances between the groups on trial 2 across the same test days when there was an interval of 60 s between trials were compared. The average path length data for trial 1 versus trial 2 (Figs. 4D and E) showed that *Fgf14*$^{-/-}$ mice had much longer average path lengths during trial 1 compared to those of WT mice, while group differences during trial 2 were much smaller. An ANOVA of these data revealed a significant main effect of Genotype for studies 1 and 2 [$F(1,20)=8.5$, $p=0.008$; and $F(1,13)=8.8$, $p=0.011$, respectively], with no other significant overall effects. Individual ANOVAs were conducted for the path length data from trials 1 and 2 to determine whether significant differences existed between groups for either trial. The results of these ANOVAs showed that for both studies 1 and 2, *Fgf14*$^{-/-}$ mice had significantly longer average path lengths relative to WT mice during trial 1 [$F(1,20)=14.4$, $p=0.001$; $F(1,13)=9.8$, $p=0.008$, respectively], while the groups did not differ significantly in average path length during trial 2. These data suggest that increasing the "memory load" for the water navigation task produced performance deficits in *Fgf14*$^{-/-}$ mice that were not demonstrable with less challenging memory demands.

Normal conditioned fear and passive avoidance performance in Fgf14$^{-/-}$ mice

To determine the generality of the spatial learning deficits, mice were tested on a step-through passive avoidance task 1 week after completion of the water maze procedures in study 1. No differences were found between *Fgf14*$^{-/-}$ and WT mice in terms of the number of trials required to reach an acquisition criterion for demonstrating learning to avoid the dark chamber associated with shock (Fig. 4F). During recall trials, *Fgf14*$^{-/-}$ mice tended to have shorter latencies for entering the dark-shock chamber compared to the WT group for both the 24 h and 48 h retention/extinction intervals, although these differences were not statistically significant (Fig. 4G). In a conditioned fear test conducted 2 months after completion of the place/probe trials in study 2B, no differences between *Fgf14*$^{-/-}$ and WT mice were observed. Statistical analysis (ANOVA) of the baseline data from min 1 and 2 on day 1 of the conditioned fear test followed by pairwise comparisons showed that *Fgf14*$^{-/-}$ and WT mice did not differ significantly in terms of percent of time spent freezing during either minute. In addition, no significant differences in freezing were observed between the groups either during the pairing of a tone (CS) with shock (US) on day 1, or on day 2 when contextual fear conditioning was evaluated (Figs. 4H and I). Also, there were no significant differences during baseline testing in an altered environment on day 3 or during auditory cue testing on that day (data not shown). The lack of significant differences between WT and *Fgf14*$^{-/-}$ mice on the passive avoidance and conditioned fear tests suggest that the deficits observed in spatial (place) learning in the water maze represent a relatively selective cognitive impairment.

Impaired theta burst induction of LTP in Fgf14$^{-/-}$ mice

To investigate whether the behavioral deficits in *Fgf14*$^{-/-}$ mice were associated with altered hippocampal synaptic plasticity, LTP was evaluated at Schaffer Collateral-CA1 synapses in

hippocampal slices using 3 theta burst stimuli (3TB) induction (Fig. 5). The amplitude of baseline fEPSP and the response to different stimulation intensities was not significantly different between WT and *Fgf14*$^{-/-}$ mice (Figs. 5A, B under Input/Output). Successful induction and maintenance of LTP was defined when at least 20% potentiation of the fEPSP slope over the baseline response was sustained 55 to 60 min after LTP induction. Successful induction and maintenance of LTP was observed in all 5 WT slices; the fEPSP slope was 158.4 ±15.1% of baseline; *n*=5 slices, 5 mice (Fig. 5A under 55–60′ post 3TB, C, D). In contrast, although there was potentiation of the fEPSP after 3TB induction in *Fgf14*$^{-/-}$ slices, the potentiation reversed approximately 40 min after LTP (Fig. 5C); the fEPSP slope was 99.6 ± 11.3% of baseline in 3 of 5 *Fgf14*$^{-/-}$ slices; *n*=3 slices, 3 mice (Fig. 5B under 55–60′ post 3TB, C, D). The difference in LTP magnitude between WT and *Fgf14*$^{-/-}$ slices, when quantified 55–60 min after 3TB (Fig. 5D), showed a statistically significant difference [$F(1,38)=37.4$, $p<0.001$. ANOVA]. Two of the five *Fgf14*$^{-/-}$ slices had reduced fEPSP slope, compared to baseline, after 3TB stimulation (not shown). These data show that FGF14 deficiency affects induction and maintenance of LTP, suggesting that impaired LTP may be associated with disrupted synaptic plasticity, which may play a role in the selective spatial memory deficits in *Fgf14*$^{-/-}$ mice.

Normal PHR and amygdala anatomy in Fgf14$^{-/-}$ mice

To determine if spatial learning/memory deficits were associated with any neuroanatomical abnormalities in *Fgf14*$^{-/-}$ mice, histochemical stains and antibodies were used to examine the anatomy and distribution of synaptic proteins in the hippocampus, PHR, and amygdala. Nissl-stained sections showed normal patterns, cytoarchitecture, and cell/neurite density in the hippocampus, in the entorhinal, perirhinal and postrhinal cortices, and in the amygdala of WT and *Fgf14*$^{-/-}$ mice (Figs. 6A, G, H). Immunohistochemical analysis of the hippocampus showed no significant differences in the distribution of glial density between WT and *Fgf14*$^{-/-}$ mice in the CA1 region (Fig. 6B). Furthermore, there were no differences in the staining intensity or expression pattern of the presynaptic proteins, SNAP-25 and synaptophysin (Figs. 6C, D), or the post-synaptic proteins, PKCγ and CaMKII (Figs. 6E and F). PKCγ and CaMKII have a critical role in LTP in the stratum pyramidal and stratum radiatum of CA1. We have also shown that hippocampal fiber tracts were not different between WT and *Fgf14*$^{-/-}$ mice using antibodies to detect synaptophysin (Schaffer collateral pathway), GAP43 (perforant pathway), or calbindin (mossy fiber projections) (Xiao et al., in press).

Discussion

In the present study we have shown that *Fgf14*$^{-/-}$ mice have reliable spatial learning deficits, further extending the similarities between *Fgf14*$^{-/-}$ mice, *FGF14(F145S)* and *FGF14 (D163fsX12)* humans. These results are consistent with other recent findings of ours relating to the neurophysiological function of FGF14 (Xiao et al., in press). Specifically, Xiao et al. demonstrated that *Fgf14*$^{-/-}$ mice exhibit decreased tetanus-induced LTP at Schaffer collateral-CA1 synapses, impaired synaptic transmission, and altered presynaptic vesicle trafficking, docking and synaptic protein expression. Here, we have replicated and extended the electrophysiological findings by demonstrating impaired theta burst induced LTP in *Fgf14*$^{-/-}$ mice and also documented FGF14 expression in brain regions thought to be involved in learning and memory, such as the hippocampus, parahippocampal region, and amygdala. Collectively, our recent findings suggest that FGF14 may play a role in mediating certain spatial learning/memory functions, possibly through modulating molecular mechanisms involved with hippocampal synaptic plasticity.

The idea that *Fgf14*$^{-/-}$ mice have reliable deficits in spatial learning is supported by the results from three water navigation experiments, each of which showed impaired acquisition

performance in *Fgf14*$^{-/-}$ mice during place trials in terms of both escape path length and latency to find the submerged platform. We replicated our initial finding of acquisition (place learning) performance deficits in *Fgf14*$^{-/-}$ mice using separate groups of naive mutant and WT mice. Furthermore, we showed that *Fgf14*$^{-/-}$ mice also exhibit impaired acquisition performance when they were retested in the water maze and required to learn another submerged platform location in the presence of different patial cues (study 2B). Comparing the results from the place and probe trials from these experiments suggest that acquisition was more severely affected than retention in *Fgf14*$^{-/-}$ mice because differences between groups were found for time in the target quadrant and average proximity scores, only during the probe trials in study 2B. However, data showing that *Fgf14*$^{-/-}$ mice exhibited impaired performance on trial 1, when the retention interval between acquisition trials was long (24 h), but performed at control-like levels when the retention interval was short (60 s), suggests that retention deficits do exist in *Fgf14*$^{-/-}$ mice but they require more challenging memory demands to be clearly demonstrable. Although *Fgf14*$^{-/-}$ mice showed reliable performance deficits in spatial learning, it is reasonable to question whether this reflects nonassociative influences or genuine cognitive impairments since we have shown in the present and previous work (Wang et al., 2002) that *Fgf14*$^{-/-}$ mice have compromised sensorimotor functions and exhibit ataxia and paroxysmal dyskinesia.

To minimize effects from paroxysmal dyskinesia, mice that were 6 to 9 months old were chosen for the two water maze studies since we had noted that episodes of paroxysmal dyskinesia were much less frequent in 6 months and older *Fgf14*$^{-/-}$ mice. In fact, only one episode of paroxysmal dyskinesia was detected in one mouse during water navigation testing, and that animal was not tested until the end of the session when it appeared to have sufficiently recovered. The most compelling evidence that *Fgf14*$^{-/-}$ mice have cognitive deficits, as well as impairments in other functions, come from data generated during the cued and place conditions within each water maze study. For example, *Fgf14*$^{-/-}$ mice and WT littermates did not differ in terms of path length in navigating to the visible platform when the mice were first introduced into the pool during the cued trials from either study 1 or 2, even though *Fgf14*$^{-/-}$ mice exhibited slower swimming speeds in study 1. In contrast, *Fgf14*$^{-/-}$ mice showed consistently increased path lengths during place trials. More importantly, in studies 2 and 2B, there were no differences between *Fgf14*$^{-/-}$ mice and WT controls in swimming speeds, yet the *Fgf14*$^{-/-}$ mice were still significantly impaired during the place trials for both path length and latency. Thus, differences in swimming speeds cannot account for the impaired performance of the *Fgf14*$^{-/-}$ mice during place trials. In addition, the heightened activity of the *Fgf14*$^{-/-}$ mice observed in both behavioral studies suggests that the inferior spatial learning performance of the *Fgf14*$^{-/-}$ mice was not likely due to general malaise or torpor associated with the mutation. In summary, ample evidence suggests that the impaired spatial learning performance in *Fgf14*$^{-/-}$ mice represents genuine cognitive impairment rather than being the result of nonassociative influences such as compromised motor or sensorimotor functions.

To determine the specificity of the cognitive deficits in *Fgf14*$^{-/-}$ mice, they were further evaluated on two non-spatial tests, step-through passive avoidance and contextual fear. The lack of significant performance deficits in *Fgf14*$^{-/-}$ mice on these tests suggests that the impaired spatial learning observed in *Fgf14*$^{-/-}$ mice was not due to global deterioration in general cognitive capabilities. These findings are particularly notable given that *Fgf14*$^{-/-}$ mice were significantly more active than WT mice and therefore would have had a greater tendency to enter the dark-shock chamber rather than avoid it. Taken together, these data suggest that functions in certain brain regions that are important for contextual learning tasks were relatively intact in *Fgf14*$^{-/-}$ mice, while functions in regions that are important for spatial learning and memory were compromised. It should also be noted that the place learning condition in the water maze is a reference memory-based task, where the hidden platform location remains the same across all trials. In rodents, reference (trial-independent) memory is often contrasted with

working (trial-dependent) memory, which involves recalling what was done on the most recent trials in order to determine a correct response for the current trial (Olton and Papas, 1979). Thus, the impairment in spatial learning in *Fgf14*$^{-/-}$ mice applies only to reference memory-related capabilities, while spatial working memory functions remain the subject for future experiments.

It was proposed in earlier theories of hippocampal function that spatial and contextual learning shared a common underlying process (O'Keefe and Nadel, 1978); however, recent studies suggest a dissociation in the neural mechanisms underlying the two types of learning (Bucci et al., 2000; Burwell et al., 2004; Peters et al., 2003). For example, damage to parahippocampal cortical regions in rats produces reliable deficits in contextual learning, while spatial (place) learning in the water maze is typically unaffected, suggesting that spatial functions may be able to operate independent of this type of information processing, particularly when distal cues are simple (Burwell et al., 2004). Our findings of spatial learning (acquisition) deficits with preserved contextual learning capabilities in *Fgf14*$^{-/-}$ mice are consistent with this model.

Results from the present and a recent study of ours (Xiao et al., in press) suggest that there are no obvious gross anatomical defects in the hippocampus, PHR, or amygdala of *Fgf14*$^{-/-}$ mice that can account for their spatial learning deficits. In contrast, we have generated ample evidence in both the present study and in Xiao et al. (Xiao et al., in press) that *Fgf14*$^{-/-}$ mice have abnormal LTP compared to WT controls. For example, we showed that LTP could not be induced or maintained in Schaffer collateral-CA1 synapses in hippocampal slices from adult *Fgf14*$^{-/-}$ mice using standard stimulation protocols (Xiao et al., in press) or theta burst protocols (Fig. 5). Alterations in basal synaptic transmission and short-term potentiation (STP), the latter being manifested in the form of attenuated post-tetanic potentiation, were also found in *Fgf14*$^{-/-}$ mice in that study. Results from the present study are in agreement with the above results in that 3TB stimulation in a similar preparation also failed to induce and maintain LTP when stimulation parameters were used that were closer to normal physiological conditions. Thus, there is strong evidence that FGF14 deficiency produces abnormalities in synaptic plasticity. In addition, Xiao et. al. observed reduced numbers of synaptic vesicles docked at presynaptic active zones, decreased spontaneous miniature synaptic current (mEPSC) frequency with normal amplitude, synaptic fatigue/depression during high/low-frequency stimulation, and decreased expression of selective synaptic proteins in *Fgf14*$^{-/-}$ mice (Xiao et al., in press). These observations suggest that FGF14 deficiency produces presynaptic dysfunction that may underlie the abnormal synaptic plasticity in *Fgf14*$^{-/-}$ mice. Although normal mEPSC amplitude in cultured hippocampal neurons from *Fgf14*$^{-/-}$ mice (Xiao et al., in press) is one indicator of normal postsynaptic AMPA receptor function, postsynaptic mechanisms contributing to impaired LTP have not been excluded. The defects in hippocampal synaptic plasticity may play a role in determining learning and memory capabilities and possibly other related cognitive/behavioral functions in *Fgf14*$^{-/-}$ mice, although altered functions in other forebrain regions normally expressing *Fgf14* may also contribute to these deficits. Our findings underscore the utility of using *Fgf14*$^{-/-}$ mice to gain a better understanding of similar functional disturbances in humans with *FGF14* mutations.

Acknowledgments

We thank L. Li, A. Saharge, A. Meyenburg and K. Johnson for excellent technical assistance. This work was supported in part by NIH grants CA60673 (D.M.O.), AG11355 (D.F.W.), funds from the Department of Molecular Biology and Pharmacology, Washington University School of Medicine and the McDonnell Foundation (K.A.Y.).

References

Brusse E, de Koning I, Maat-Kievit A, Oostra BA, Heutink P, van Swieten JC. Spinocerebellar ataxia associated with a mutation in the fibroblast growth factor 14 gene (SCA27): A new phenotype. Mov. Disord 2006;21:396–401. [PubMed: 16211615]

Bucci DJ, Phillips RG, Burwell RD. Contributions of postrhinal and perirhinal cortex to contextual information processing. Behav. Neurosci 2000;114:882–894. [PubMed: 11085602]

Burwell RD, Saddoris MP, Bucci DJ, Wiig KA. Corticohippocampal contributions to spatial and contextual earning. J. Neurosci 2004;24:3826–3836. [PubMed: 15084664]

Connolly AM, Keeling RM, Mehta S, Pestronk A, Sanes JR. Three mouse models of muscular dystrophy: the natural history of strength and fatigue in dystrophin-, dystrophin/utrophin-, and laminin alpha2-deficient mice. Neuromuscul. Disord 2001;11:703–712. [PubMed: 11595512]

Dalski A, Atici J, Kreuz FR, Hellenbroich Y, Schwinger E, Zuhlke C. Mutation analysis in the fibroblast growth factor 14 gene: frameshift mutation and polymorphisms in patients with inherited ataxias. Eur. J. Hum. Genet 2005;13:118–120. [PubMed: 15470364]

Diano S, Farr SA, Benoit SC, McNay EC, da Silva I, Horvath B, Gaskin F, Nonaka S, Jaeger N, Banks LB, et al. Ghrelin controls hippocampal spine synapse density and memory performance. Nat. Neurosci 2006;9:381–388. [PubMed: 16491079]

Gallagher M, Burwell R, Burchinal M. Severity of spatial learning impairment in aging: development of a learning index for performance in the Morris water maze. Behav. Neurosci 1993;107:618–626. [PubMed: 8397866]

Grady RM, Wozniak DF, Ohlemiller KK, Sanes JR. Cerebellar synaptic defects and abnormal motor behavior in mice lacking alpha- and beta-dystrobrevin. J. Neurosci 2006;26:2841–2851. [PubMed: 16540561]

Ho N, Liauw JA, Blaeser F, Wei F, Hanissian S, Muglia LM, Wozniak DF, Nardi A, Arvin KL, Holtzman DM, et al. Impaired synaptic plasticity and cAMP response element-binding protein activation in Ca2+/calmodulin-dependent protein kinase type IV/Gr-deficient mice. J. Neurosci 2000;20:6459–6472. [PubMed: 10964952]

Khuchua Z, Wozniak DF, Bardgett ME, Yue Z, McDonald M, Boero J, Hartman RE, Sims H, Strauss AW. Deletion of the N-terminus of murine map2 by gene targeting disrupts hippocampal ca1 neuron architecture and alters contextual memory. Neuroscience 2003;119:101–111. [PubMed: 12763072]

Lou JY, Laezza F, Gerber BR, Xiao M, Yamada KA, Hartmann H, Craig AM, Nerbonne JM, Ornitz DM. Fibroblast growth actor 14 is an intracellular modulator of voltage-gated sodium channels. J. Physiol 2005;569:179–193. [PubMed: 16166153]

Magnusson KR. Aging of glutamate receptors: correlations between binding and spatial memory performance in mice. Mech. Ageing Dev 1998;104:227–248. [PubMed: 9818728]

Munoz-Sanjuan I, Smallwood PM, Nathans J. Isoform diversity among fibroblast growth factor homologous factors is generated by alternative promoter usage and differential splicing. J. Biol. Chem 2000;275:2589–2597. [PubMed: 10644718]

Nabeshima T, Noda Y, Mamiya T. The role of nociceptin in cognition. Brain Res 1999;848:167–173. [PubMed: 10612708]

O'Keefe, RJ.; Nadel, L. The Hippocampus as a Cognitive Map. Oxford: Oxford Univ. Press; 1978.

Olton DS, Papas BC. Spatial memory and hippocampal function. Neuropsychologia 1979;17:669–682. [PubMed: 522981]

Peters M, Mizuno K, Ris L, Angelo M, Godaux E, Giese KP. Loss of Ca2+/calmodulin kinase kinase beta affects the formation of some, but not all, types of hippocampus-dependent long-term memory. J. Neurosci 2003;23:9752–9760. [PubMed: 14586002]

Schaefer ML, Wong ST, Wozniak DF, Muglia LM, Liauw JA, Zhuo M, Nardi A, Hartman RE, Vogt SK, Luedke CE, et al. Altered stress-induced anxiety in adenylyl cyclase type VIII-deficient mice. J. Neurosci 2000;20:4809–4820. [PubMed: 10864938]

Smallwood PM, Munoz-Sanjuan I, Tong P, Macke JP, Hendry SH, Gilbert DJ, Copeland NG, Jenkins NA, Nathans J. Fibroblast growth factor (FGF) homologous factors: new members of the FGF family implicated in nervous system development. Proc. Natl. Acad Sci. U. S. A 1996;93:9850–9857. [PubMed: 8790420]

Van Swieten JC, Brusse E, De Graaf BM, Krieger E, Van De Graaf R, De Koning I, Maat-Kievit A, Leegwater P, Dooijes D, Oostra BA, Heutink P. A mutation in the fibroblast growth factor 14 gene is associated with autosomal dominant cerebellar ataxia. Am. J. Hum. Genet 2003;72:191–199. [PubMed: 12489043]

Wang Q, McEwen DG, Ornitz DM. Subcellular and developmental expression of alternatively spliced forms of fibroblast growth factor 14. Mech. Dev 2000;90:283–287. [PubMed: 10640713]

Wang Q, Bardgett ME, Wong M, Wozniak DF, Lou J, McNeil BD, Chen C, Nardi A, Reid DC, Yamada K, Ornitz DM. Ataxia and paroxysmal dyskinesia in mice lacking axonally transported FGF14. Neuron 2002;35:25–38. [PubMed: 12123606]

Wozniak DF, Hartman RE, Boyle MP, Vogt SK, Brooks AR, Tenkova T, Young C, Olney JW, Muglia LJ. Apoptotic neurodegeneration induced by ethanol in neonatal mice is associated with profound learning/memory deficits in juveniles followed by progressive functional recovery in adults. Neurobiol. Dis 2004;17:403–414. [PubMed: 15571976]

Xiao M, Xu L, Laezza F, Yamada K, Feng S, Ornitz DM. Impaired hippocampal synaptic transmission and plasticity in mice lacking fibroblast growth factor 14. Mol. Cell Neurosci. in press

Yamada KA, Rensing N, Izumi Y, De Erausquin GA, Gazit V, Dorsey DA, Herrera DG. Repetitive hypoglycemia in young rats impairs hippocampal long-term potentiation. Pediatr. Res 2004;55:372–379. [PubMed: 14681492]

Yamamoto S, Mikami T, Ohbayashi N, Ohta M, Itoh N. Structure and expression of a novel isoform of mouse FGF homologous actor (FHF)-4. Biochim. Biophys. Acta 1998;1398:38–41. [PubMed: 9602045]

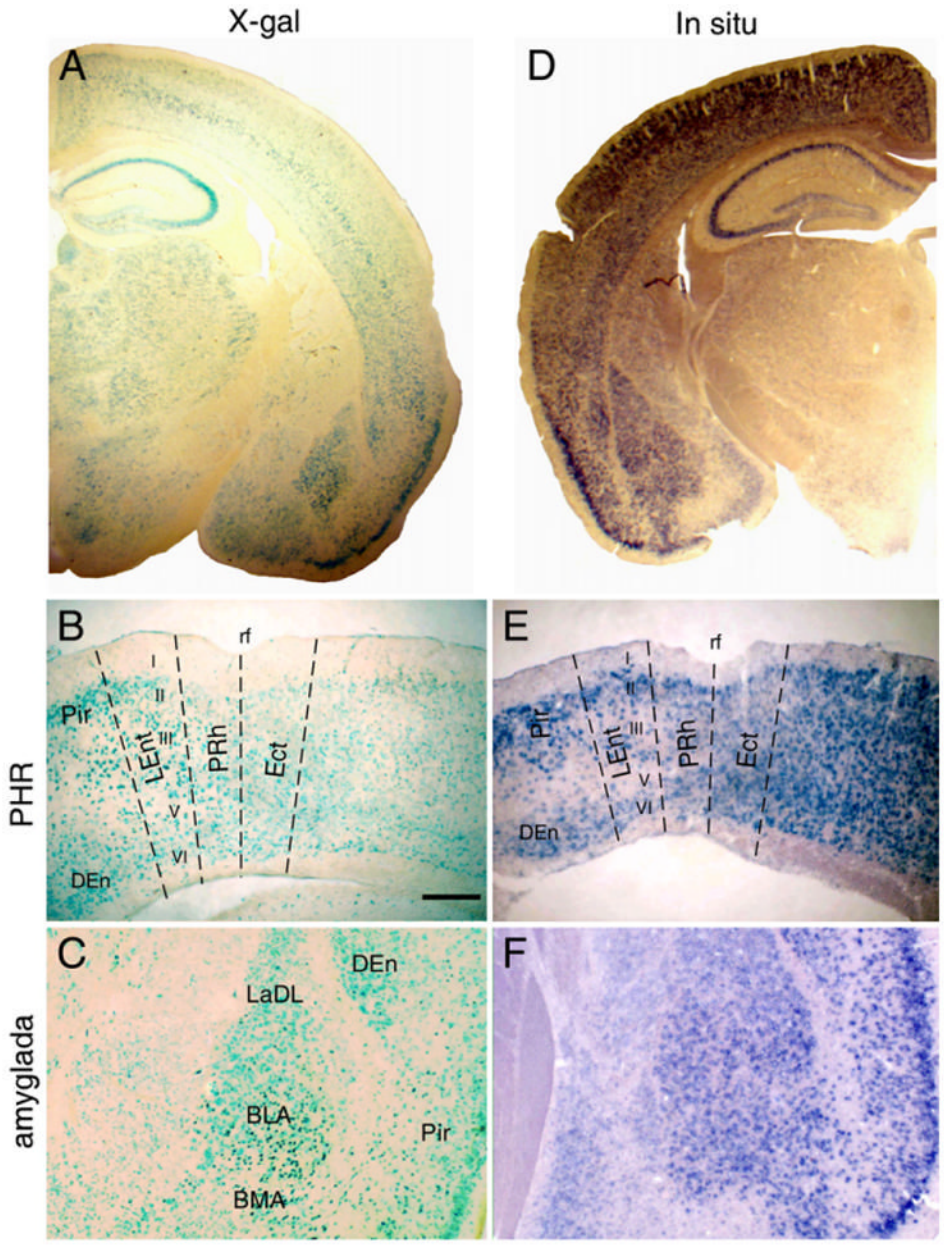

Fig. 1.

FGF14 expression in hippocampus and PHR. (A) FGF14-β-gal expression in the forebrain. (B) FGF14-β-gal expression in the PHR (PRh, LEnt, medial entorhinal cortex), Pir and DEn showing expression in neurons in layers II, III, V and VI of the PRh in *Fgf14*$^{-/+}$ mice. (C) FGF14-β-gal expression in major nuclei of the amygdala. (D) In situ detection of *Fgf14* in the forebrain. (E) FGF14-β-gal expression in the PHR showing similar patterns of expression to that of FGF14-β-gal. (F) *Fgf14* mRNA expression in the amygdala showing a similar expression pattern to FGF14-β-gal. BLA, anterior basolateral amygdaloid nucleus; BMA, anterior basolateral amygdala; DEn, dorsal endopiriform nucleus; LaDL, dorsolateral amygdaloid nucleus; LEnt, lateral entorhinal cortex; Pir, piriform cortex; PRh, perirhinal cortex; rf, rhinal fissure. Bar=200 μm.

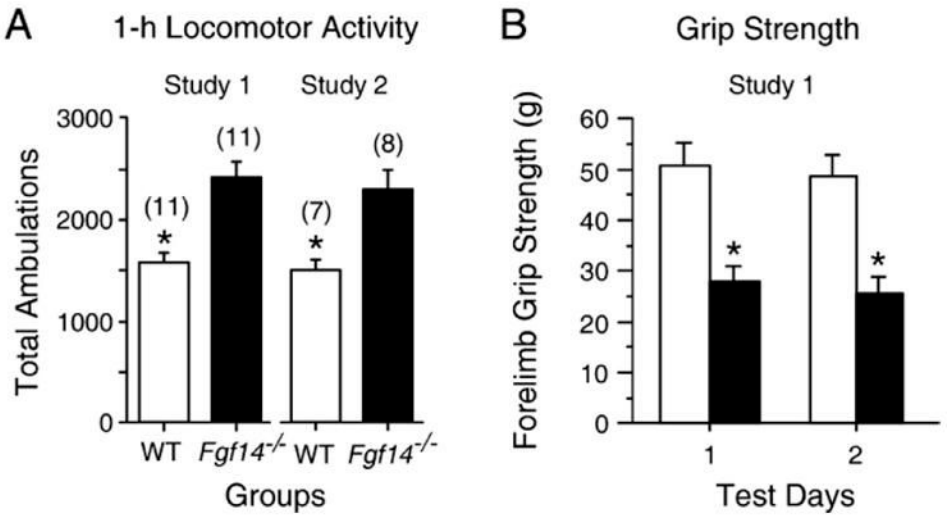

Fig. 2.

Fgf14$^{-/-}$ mice exhibited hyperactivity and impaired grip strength. (A) *Fgf14*$^{-/-}$ mice exhibited significantly more total ambulations (mean±SEM, *, $p<0.005$) during 1-h locomotor activity tests relative to WT littermate controls in both study 1 and study 2, providing good evidence that the *Fgf14*$^{-/-}$ mice are hyperactive. (B) *Fgf14*$^{-/-}$ mice demonstrated impaired forelimb grip strength relative to WT control mice on both Test Day 1 and Day 2 ($p<0.0005$; $p<$Bonferroni corrected $p=0.025$).

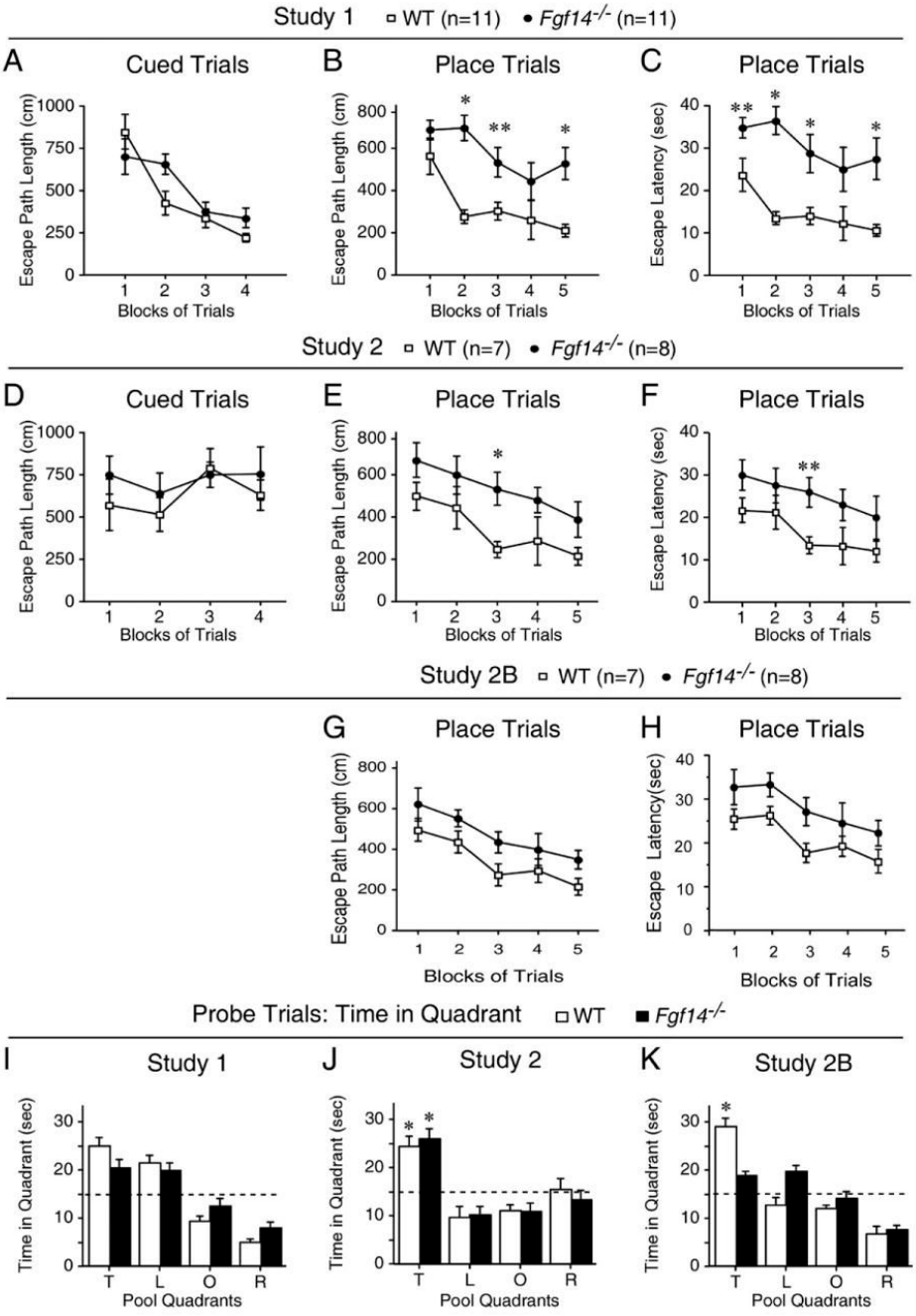

Fig. 3.

Fgf14$^{-/-}$ mice have impaired spatial learning as evaluated by the water navigation test. (A) In study 1, *Fgf14*$^{-/-}$ mice did not differ significantly from WT littermate controls in terms of escape path length (mean±SEM) during cued (visible platform) trials. (B) In contrast to the lack of group differences in the cued trials data, *Fgf14*$^{-/-}$ mice exhibited significantly impaired acquisition performance in terms of escape path length (mean±SEM) during place (submerged platform) trials compared to WT controls. *p<0.001 (Bonferroni corrected p=0.01), **p=0.011. (C) The *Fgf14*$^{-/-}$ mice also exhibited significantly impaired acquisition performance in terms of escape latency (mean±SEM) during place trials compared to WT controls. *p<0.003, **p=0.03. (D) Similar to the cued trials results in study 1, *Fgf14*$^{-/-}$ mice

in study 2 did not differ significantly from WT littermate controls in terms of escape path length (mean±SEM) during cued trials. (E) The acquisition performance of the *Fgf14*$^{-/-}$ mice in study 2 was impaired during place trials in terms of path length (mean±SEM), which was also consistent with the place trials data from study 1. *p=0.007. (F) The *Fgf14*$^{-/-}$ mice also demonstrated performance deficits during place trials in study 2 in terms of escape latency (mean±SEM). **p=0.011. (G, H) A significant main effect of genotype was found for both path length (G) and latency (H), [F(1,13)=9.3, p=0.009; and F(1,13)=5.9, p=0.03, respectively], for study 2B, thus documenting generally-impaired performance across blocks of trials on the part of the *Fgf14*$^{-/-}$ mice to learn new platform locations. (I) Retention performance during the probe trial in study 1 was not highly "resolved" in either the *Fgf14*$^{-/-}$ or WT groups since neither showed a "spatial bias" for the target quadrant (increased time spent in the target quadrant versus time in each of the other quadrants). (J) In contrast, both the *Fgf14*$^{-/-}$ and WT mice showed a spatial bias for the target quadrant in study 2, where each group spent significantly (*p<0.003) more time in the target quadrant compared to each of the other quadrants. (K) However, when the same mice were required to learn a new platform location during the place trials in study 2B, only the WT mice showed a significant spatial bias for the target quadrant during the probe trial. *p<0.002. Pool Quadrants: T=target quadrant that contained the platform; L=quadrant to the left of the target quadrant; O=quadrant opposite the target quadrant; R=quadrant to the right of the target quadrant.

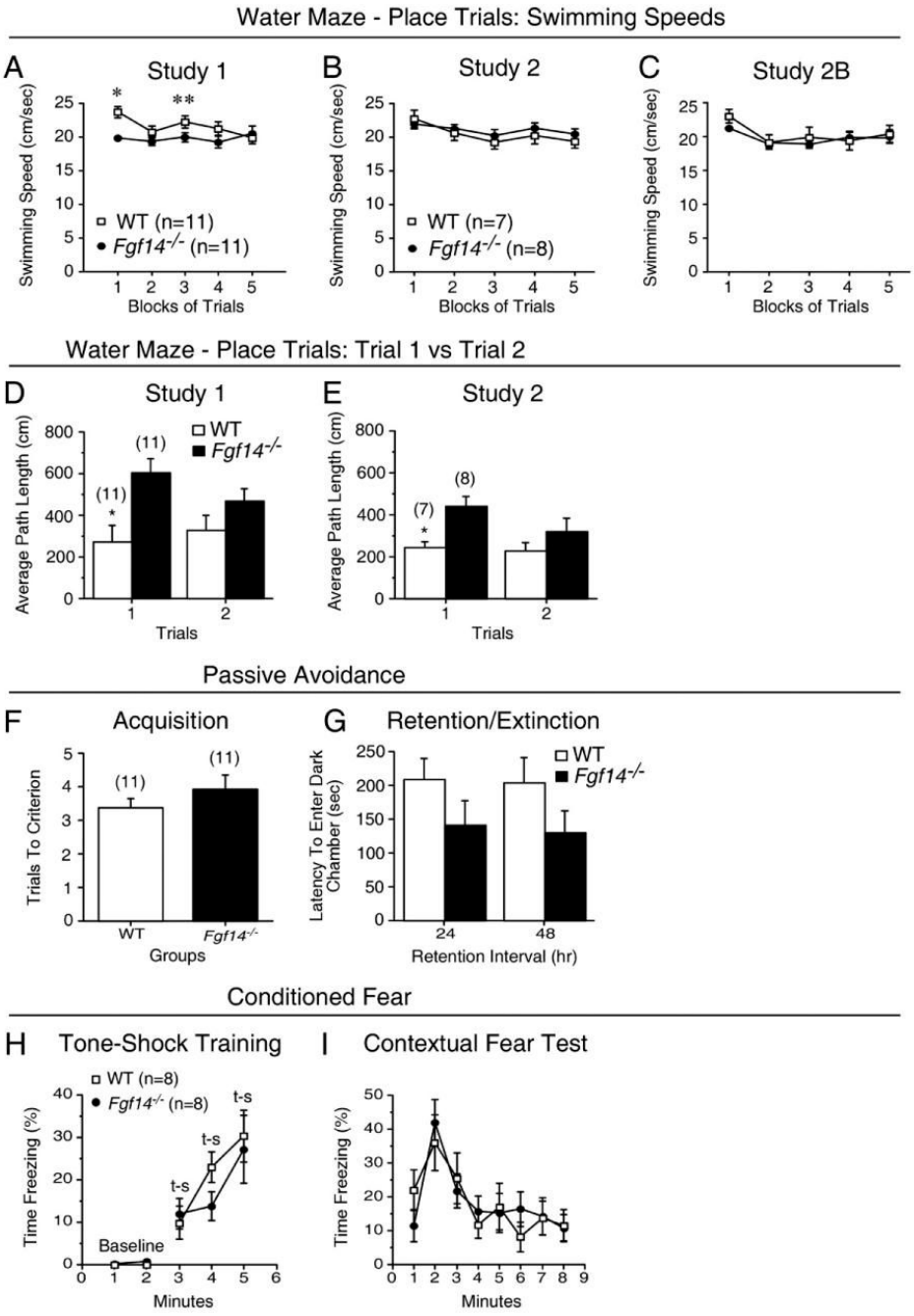

Fig. 4.

Swimming speeds, retention deficits and normal passive avoidance and conditioned fear performance in *Fgf14*$^{-/-}$ mice. (A) A significant genotype by blocks of trials interaction and subsequent contrasts pertaining to the swimming speeds data from the place trials in study 1 suggested that the *Fgf14*$^{-/-}$ mice were slower than the WT mice early in acquisition training but that similar speeds were observed in the two groups at the end of training. **p*=0.0005; ***p*=0.046. (B) In contrast, no differences in swimming speeds were observed between groups during the place trials in study 2, suggesting that compromised swimming abilities were not responsible for the impaired spatial learning performance in *Fgf14*$^{-/-}$ mice. (C) The swimming speeds of *Fgf14*$^{-/-}$ and WT mice were also found not to differ during the place trials in study

2B when the mice were required to learn a new submerged platform location. (D, E) *Fgf14*$^{-/-}$ mice exhibited significant (*) impairment compared to WT controls on trial 1 but not trial 2 in terms of path length to the submerged platform averaged across test days during place trials in both study 1 (D) and study 2 (E) (p=0.001 and 0.008, respectively). The memory demands present during trial 1 were greater than those present for trial 2 since there was an interval of 24 h between acquisition trials with respect to trial 1, whereas only 60 s intervened between acquisition trials for trial 2. (F) *Fgf14*$^{-/-}$ mice did not differ significantly from WT controls in trials to criterion (mean±SEM) during passive avoidance acquisition in study 1. (G) Although the latencies (mean±SEM) to enter the dark-shock chamber tended to be shorter for the *Fgf14*$^{-/-}$ mice, they were not significantly different from WT controls when tested 24 h (retention) or 48 h (extinction) after passive avoidance acquisition. (H) A significant main effect of genotype [F(1,14)=6.6, p=0.02] was found on the baseline data from min 1 and 2 during day 1 of conditioned fear testing. However, subsequent pairwise comparisons showed that the *Fgf14*$^{-/-}$ mice and WT littermate controls did not differ significantly in the percent of time spent freezing (mean±SEM) for either minute. In addition, no significant differences were observed between *Fgf14*$^{-/-}$ mice and WT controls in the percent of time spent freezing (mean ±SEM) during CS-US [t-s (tone-shock)] training for min 3 to 5. (I) *Fgf14*$^{-/-}$ mice also did not differ significantly from WT controls (mean±SEM) in percent of time freezing during the contextual fear test conducted 24 h after tone-shock training when the mice were placed back into the same chamber.

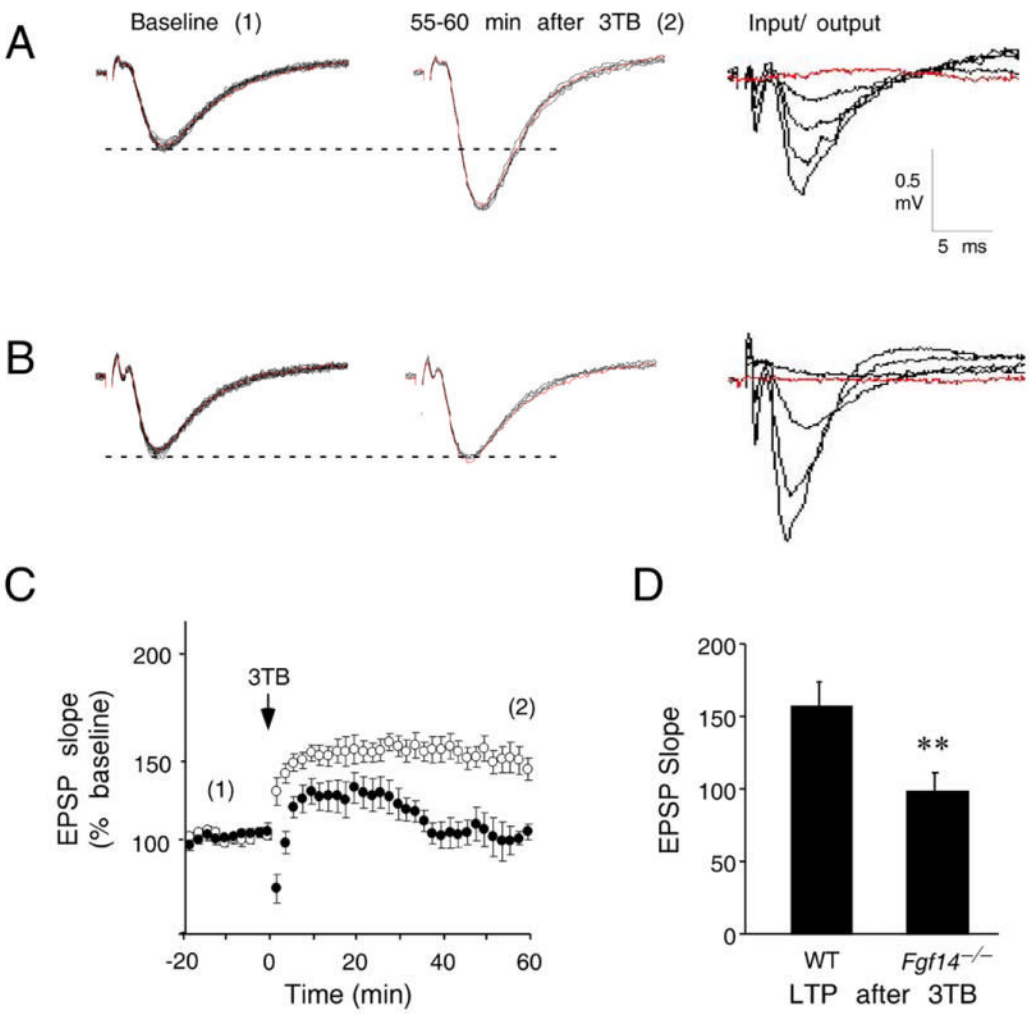

Fig. 5.

Impaired Schaffer Collateral LTP in *Fgf14*$^{-/-}$ mice. (A) Representative recordings from a hippocampal slice from a WT mouse exhibit stable fEPSP baseline responses to stimuli applied every minute for 20 min (labeled Baseline, 20 consecutive traces superimposed, red line indicates the first response). 55–60 min after 3 applications of theta burst stimuli (3TB), the fEPSP slope remains significantly potentiated relative to the baseline responses, indicating successful induction and maintenance of LTP (middle panel labeled 55–60 min after 3TB). The fEPSP shows a normally graded increase in amplitude with increasing stimulus intensity (0–250 mA stimulus, labeled Input/Output). (B) Representative recordings from a hippocampal slice from an *Fgf14*$^{-/-}$ mouse exhibit stable baseline responses (Baseline), normal input output responses (Input/Output), but failed to maintain LTP (55–60 min after 3TB). (C) Cumulative data from LTP experiments from all slices were combined by normalizing fEPSP slopes to the baseline responses. Numbers in parentheses indicate when representative traces in A and B were obtained (1, Baseline; 2, 55–60 min after 3TB). The arrow indicates when 3TB were applied. Approximately 58% potentiation of the baseline response was observed in the WT slices (open circles). Although there is initially some post 3TB potentiation, LTP is not maintained in slices from *Fgf14*$^{-/-}$ mice (closed circles). (D) LTP compared between WT and *Fgf14*$^{-/-}$ slices at 55–60 min after 3TB (corresponding to 2 in C) demonstrates impaired LTP maintenance in *Fgf14*$^{-/-}$ mice (p<0.001 one-way ANOVA). Scale bar, 0.5 mV and 5 ms. (For

interpretation of the references to colour in this figure legend, the reader is referred to the web version of this article.)

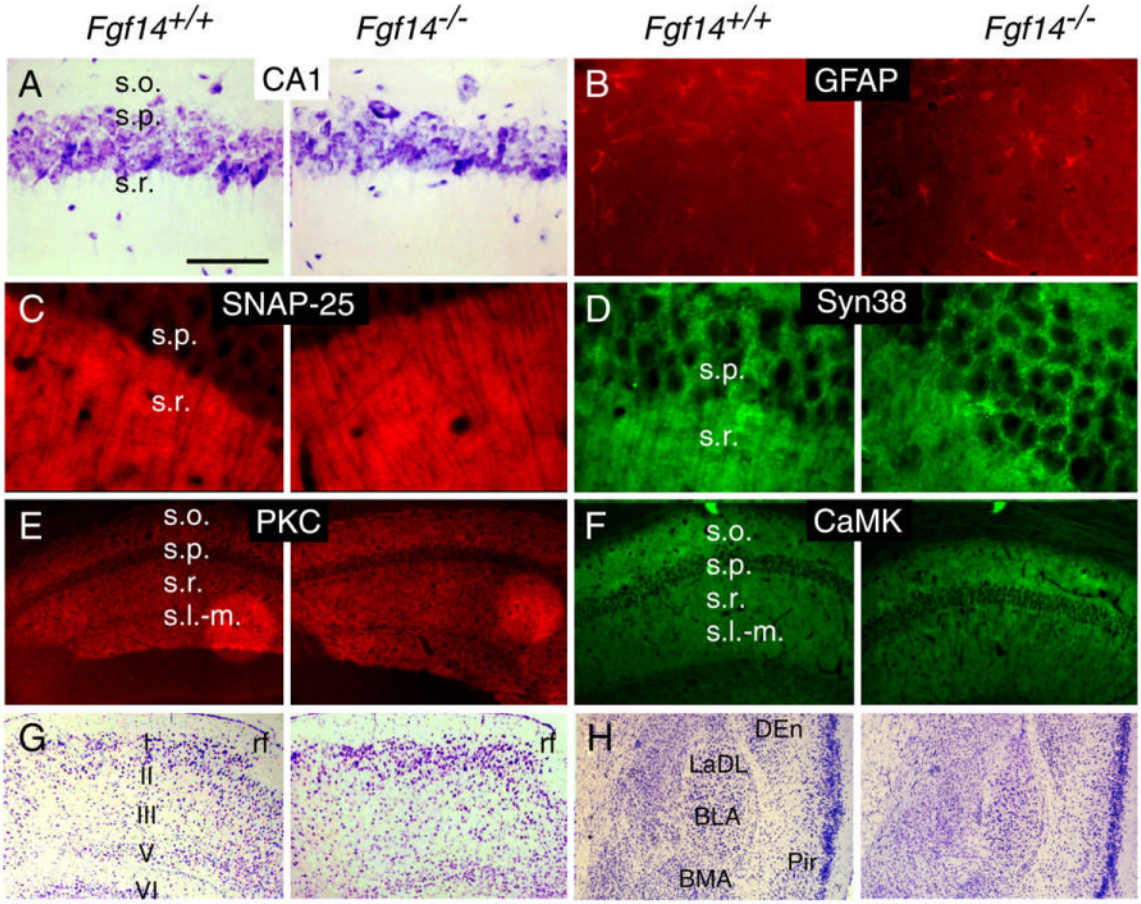

Fig. 6.

Normal PHR and amygdala anatomy in *Fgf14*$^{-/-}$ mice. (A) Normal hippocampal cytoarchitecture in the s.o., s.p. and s.r. of CA1 revealed by Nissl staining in *Fgf14*$^{-/-}$ and WT mice. (B–F) No difference was observed in the staining intensity of GFAP (B), SNAP-25 (C), Synaptophysin (Syn38) (D), PKCγ (E) and CaMKII (F) in CA1 regions of *Fgf14*$^{-/-}$ and WT mice. (G–H) Normal cytoarchitecture in the entorhinal cortex (G) and amygdala (H) in WT and *Fgf14*$^{-/-}$ mice (Nissl stain). BLA, anterior basolateral amygdaloid nucleus; BMA, anterior basolateral amygdala; LaDL, dorsolateral amygdaloid nucleus DEn, dorsal endopiriform nucleus; Pir, piriform cortex; rf, rhinal fissure; s.l-m., stratum lacunosum moleculare; s.o., stratum oriens; s.p., stratum pyramidal; s.r., stratum radiatum. Bar=125 μm (A, B); Bar=50 μm (C, D); Bar=500 μm (E–H).